Document Restoration Using 3D Shape:
A General Deskewing Algorithm for Arbitrarily Warped Documents *

Michael S. Brown and W. Brent Seales
Department of Computer Science
University of Kentucky
Lexington, KY 40506 USA

Abstract

We present a framework for restoring arbitrarily warped and deformed documents to their original planar shape. The impetus for this work is the need for tools and techniques to help digitally preserve and restore fragile manuscripts. Current digitization is performed under the assumption that the documents are flat, with subsequent image-processing and restoration algorithms either relying on this assumption or attempting to overcome it without shape information. Although most manuscripts were originally flat, many become deformed from damage and deterioration. Physical flattening is not possible without risking further, possibly irreversible, damage.

Our framework addresses this restoration problem with two primary contributions. First, we present a working 3D digitization setup that acquires a 3D model with accurate shape-to-texture registration under multiple lighting conditions. Second, we show how the 3D model and a mass-spring particle system can be used together as a framework for digital flattening. We show that this restoration process can correct document deformations and can significantly improve subsequent document analysis.

1 Introduction

Most new documents are electronically prepared and can be stored directly in a digital archive for reference, search, and distribution. Our libraries, however, are far from all-digital, and significant efforts are underway to digitize physical materials [15]. Most materials are digitized solely for the purpose of subsequent processing, such as optical character recognition (OCR) algorithms [12], and the original images are often discarded. Yet, libraries everywhere preserve historically significant and in some cases badly deteriorated documents, which carry an importance beyond the content of the words. For these collections, the *primary* purpose of digitization is the image itself, which serves as a photo-realistic facsimile. Pre-typeset materials, such as handwritten documents and any materials where there is a desire to preserve "look and feel" fall into this category.

Document imaging systems largely make the assumption that documents are flat and positioned parallel to the optical axis of the imaging sensor. In their original state, most documents indeed are flat, and this assumption holds. Older materials, however, such as those typically found in special collections (e.g., manuscripts and letters) suffer from deterioration that affects shape; this is especially true for materials made of vellum[1].

In this paper we address two key problems. First, any serious effort to preserve and disseminate *quality* electronic facsimiles of materials should recover and preserve the underlying 3D shape when appropriate. Not all manuscripts benefit from a shape analysis, but some of the most damaged, sacred, difficult texts, can benefit enormously from an accurate representation of shape. In particular, it may be difficult for a scholar to determine from an image if markings in a manuscript were created by the original author or are ambiguous distortions caused by the manuscript's underlying shape. Moreover, automatic segmentation algorithms, such as those that find staff lines in music or lines of text in handwritten materials [11], suffer as a result of the arbitrary skewing due to shape deformations. Second, while the threat of further physical deterioration makes it almost impossible to physically flatten or alter the manuscript itself, a *digital restoration* is possible. We show how to formulate this distortion removal, or "flattening" problem, providing scholars with new tools for visualization and restoration.

We are developing these tools for use with older scholarly materials, but the framework allows for a general *deskewing* processing step that can be applied in any document processing context. For example, images from bound materials where the curvature of the binding causes distortion, modern documents damaged as a result of water and fire damage or simply from improper handling, can also benefit from restoration and pre-processing techniques within our framework.

*We gratefully acknowledge support for this work by the NSF DLI-2 award #9817483.

[1] Parchment made of animal skin

The remainder of this paper develops our framework by first describing our 3D acquisition system (Section 2) for recovering and registering manuscript shape and texture under various lighting conditions. Section 3 describes the mass-spring particle system used to model and flatten the non-planar surface. Section 4 presents quantitative restoration results from controlled test cases using materials whose shape has been altered and then recovered. Section 5 concludes by summarizing our results.

2 3D Acquisition

Generally, the only pre-processing of images for automated document analysis are planar "deskewing" algorithms, which try to orient the document so that the textual contents are aligned with the raster representation [4, 6]. These algorithms assume the document is planar. Wada et al. [18] presented a technique that used inter-reflections to correct for the non-planar distortions on pages of a curved book digitized by a scanner. This shape-from-shading approach is formulated for the specific concave shape that is typical of the distortion caused by book bindings. Our goal is a general approach to the deskewing problem for any *arbitrarily* warped document. Our assumption is that the document was *originally* flat, but has become non-planar over time. The goal is to work from an accurate 3D model of the document.

Shape acquisition serves two functions. First, the data will be used as input to the restoration framework. Second, for the purpose of careful scholarly analysis and accurate preservation, the 3D representation is a more useful metric facsimile, which gives the true "look and feel" beyond that of a single 2D image.

2.1 Structured Light

A number of possible approaches can be applied to acquire 3D representations of documents. Our system satisfies a set of design goals peculiar to the domain of manuscript analysis, existing digitization paradigms within libraries, and the capabilities of library staff:

Multiple lighting conditions: For many manuscripts it is desirable to recover images under a variety of different lighting conditions. For example, it is common to collect images under illumination from natural light, white light, ultra-violet light, and fiber-optic backlighting. Each of these lighting techniques has been successful for enhancing erased text and various portions of severely damaged texts that are hidden by misguided restoration schemes (gauze, tape, paper frames) [13]. The 3D acquisition technique must allow these multiple images to be registered accurately to the acquired 3D model.

Capital costs and existing framework: Lower cost means wider acceptance and ability within restricted budgets to provide the necessary equipment. Costs combined with the ability to inter-operate with existing digitization hardware (camera, gantry, computer hardware support) were a major design consideration.

Staff capability: While the computer-trained *digiteur* as a staff position is emerging in a number of libraries, it is still the case that most digitization efforts are led by non-expert computer users who cannot be expected to perform difficult and expert software and hardware manipulations. The acquisition system is designed to be used by non-experts.

Given these considerations, we designed and implemented a structured light (SL) approach using a commercially available off-the-shelf projector as the light source[2, 3]. SL integrated well with existing 2D digitization setups by using the existing high-resolution camera. By augmenting rather than replacing the setup, we did not require additional space. The system also allows the curator the option of acquiring or not acquiring 3D for each document instance without a setup change. Since the existing camera is already driven by a PC, the only additional hardware required is a standard XGA light projector. Figure2.1(a) shows a typical setup.

2.2 Device Calibration

The projector and camera are fully calibrated using known methods [5]. This involves constructing a calibration pattern with known spatial features and determining where these 3D features appear in the image plane of both the camera and the projector. Our physical pattern (checker board) has spatial features that span the depth of field of the documents to be scanned. We use a *Kitchen-Rosenfeld*[10] corner detector to obtain sub-pixel feature measurements (0.1 pixel accuracy). The camera is calibrated by capturing images of the pattern and detecting corners. The projector is calibrated indirectly via the camera, which observes points projected onto the calibration pattern.

2.3 3D Model Reconstruction

The particular strength of the SL approach is the ability to obtain robust and accurate point correspondences between devices. There are a myriad of ways to expedite the detection of these correspondences: active encoding schemes using gray-coding, phase-modulation, etc. [7]. In order to achieve simplicity and accuracy, we use a striping approach, in which the camera observes the document as the projector sweeps a vertical or horizontal line across it. This approach sacrifices speed but produces very accurate results. Synchronization is performed by controlling the camera and projector from the same computer. As each line is projected from the projector, it is observed in the camera as a curve that is warped by the object's shape. Outliers are

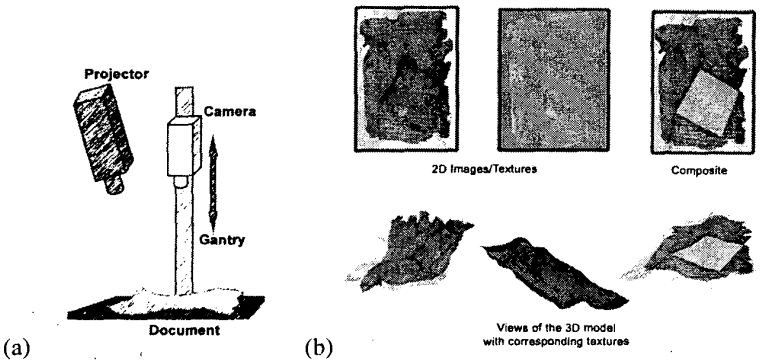

Figure 1: (a) A typical 2D manuscript digitization setup places a camera mounted on a gantry perpendicular to a flat bed onto which the document is placed. The gantry allows the camera to be positioned. This setup can be converted into a 3D imaging setup with the addition of a light projector. (b) Any number of images of a manuscript can be captured and used as textures for a single 3D model. Using the same camera for reconstruction and imaging makes the registration of textures to the acquired 3D shape (and texture composition) simple.

culled using epipolar constraints for the two devices. Points along this curve, which is swept over the entire document, are reconstructed in the world coordinate frame.

The SL algorithm creates a set of 3D points in the world coordinate frame (defined by the calibration pattern), sampled at the resolution of the camera, across the surface of the document. This representation is converted to a depth map in the camera's coordinate frame, from which 3D meshes (models) at user-specified resolution can easily be generated.

2.4 Texture Registration

The 3D model is textured with a 2D image captured from the same camera used to recover the 3D information. After model acquisition, any number of *texture* images can be acquired. Because the imaging device is the same optical path as the depth reconstruction device, all images captured will be registered to the 3D model (assuming that the manuscript and camera do not move). This allows for efficient creation of 3D models under different lighting conditions. Figure 2.1(b) shows an example: because the textures are automatically registered, they can easily be combined to create new textures.

2.5 Accuracy Estimation

Measuring the accuracy of the 3D acquisition system is not trivial. Common approaches to these measurements rely on the reconstruction and registration of known, machined 3D objects. In order to enable curators to gauge the accuracy of their setup (and perhaps store that information as *meta-data* with the acquired model), we measure accuracy by reconstructing a plane. The orientation of the plane is unknown, so we use the fact that the object is known to be planar. A best-fit plane is found for the recovered 3D points, and the deviation of the 3D points from this plane is calculated. Several reconstructions are made of the plane at varying orientations, with the average deviation from all the planes being used as the accuracy estimate. As we report in Section 4, we estimate accuracies of 0.25mm to 0.5mm for our setups using this estimation approach.

3 3D Model Restoration: Flattening

Our framework for digitally restoring, or flattening, 3D models of documents is a physically based modeling approach in the vein of work by *Terzopoulos et al.* [17, 16], which can model both elastic and inelastic deformations. The techniques we employed are most often applied in computer graphics and visualization applications to model change in the *appearance* of dynamically deformable materials. Our goal can be cast as the inverse problem, where a complex shape must be deformed to a plane subject to a set of material constraints that are based on the composition of the document.

As shown by our controlled results, restoration with this technique is very accurate when documents have been deformed under processes such as rigid crumpling. For a decaying manuscript, however, it may be impossible to model all of the physical phenomena that resulted in its current state. In these cases we are interested in manipulating the model in a reasonable and flexible way to help restore the *perceptual* quality of the digital representation. Moreover, this technique may be used with constraints supplied from expert scholars, whose knowledge about letter forms, for example, may provide a strong constraint to the system that can guide in making the manuscript more readable and accessible. The mass-spring system generates the desired outcomes for rigidly deformed documents, and simultaneously allows for flexibility in manipulating more complex, un-

known deformations.

3.1 Mass-Spring Particle System

A particle system is governed by the classic second order Newtonian equation, $f = ma$, where f is a force, m is the mass of a particle, and a is its acceleration. This is also commonly written as: $\ddot{x} = f/m$. A particle modeled by this equation can be described with six variables, $[x_1, x_2, x_3, v_1, v_2, v_3]$, where x_i represents the particle's 3-space position, and v_i represents its velocity. This position/velocity product space is referred to as the *phase space*. The phase space derivative with respect to time, and the subsequent motion equation, is $[v_1, v_2, v_3, f_1/m, f_2/m, f_3/m]$. This system describes a particle's mass, position and velocity at a given instant in time. Dynamic forces can be exerted on these particles over time, and new positions are calculated at advancing time intervals.

In a basic particle system, individual particles respond only to *external* forces, and have no influence on other particles. This basic system can be extended to incorporate forces between particles. One common extension, referred to as a mass-spring particle system, arises by logically connecting particles together via springs. The resulting forces on such a system can be categorized into two types: *internal*, or forces between particles; and *external* forces. The slightly modified equation expressing this is: $F_{int} + F_{ext} = ma$. In the following sections we explain the particulars of the particle system used in our experiments (for more information on physically-based modeling, see [9]).

3.2 Internal Forces

3.2.1 Ideal Hookian Spring

The internal forces in our system are due to particles connected via springs. Using Hook's law, the equations for forces between two particles, a and b are:

$$f_a = \left[k_s(|\vec{x_a} - \vec{x_b}| - r) + k_d \frac{\vec{v_a} - \vec{v_b} \cdot \vec{x_a} - \vec{x_b}}{|\vec{x_a} - \vec{x_b}|} \right] \frac{\vec{x_a} - \vec{x_b}}{|\vec{x_a} - \vec{x_b}|} \quad (1)$$

$$f_b = -f_a \quad (2)$$

where f_a and f_b are the forces on a and b, r is the rest length of the spring, $\vec{x}$ and $\vec{v}$ are the position and velocity vectors from a particle's current phase space state, k_s and k_d are the spring stiffness and damping constants, respectively, and $|\cdot|$ is the l_2 norm. It is apparent from the equations that when the system is at rest, the springs exert no force. When external forces begin to move the individual particles from their resting state, internal spring forces are induced.

3.2.2 Finite Elements

Figure 2 shows the finite elements of the mass-spring model. For each quadrangle springs are attached. Using Provot's

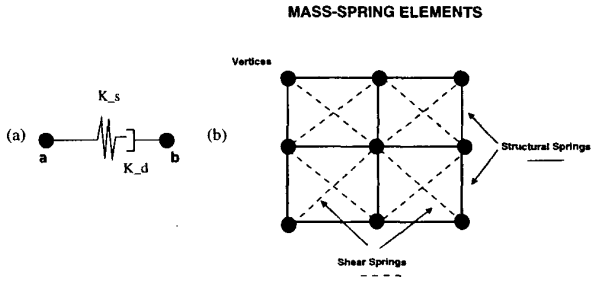

Figure 2: (a) The ideal Hookian spring with damper acts on two particles. K_s is the stiffness coefficient of the spring, and K_d is the dampening coefficient. (b) The finite element structure of the particles consists of structural and shear springs.

[14] naming convention, each element is composed of *structural* springs, which form the quadrangles' hull, and two *shear* springs, which connect diagonally. This structure is robust for modeling flexible sheet materials, such as cloth. More springs may be used to create additional rigidity if required [14].

3.3 External Forces

3.3.1 Global Downward Force and Damping

A global downward force is exerted on all particles, forcing them toward the $Z = 0$ plane[2] This force is typically modeled as a constant force, such as gravity, and can be represented as $f = mg$. In addition to a global downward force, a *viscous drag* is applied in the form $f = -\mu_d v$, where μ_d is the drag coefficient and v is the velocity state of a particle. This force encourages a particle to come to rest, and improves the numerical stability of the system.

3.3.2 Plane Collision

The goal of "flattening" is to push the 3D shape to the $Z = 0$ plane. When the x_3 phase space component of a particle is equal to 0, it has collided with the $Z = 0$ plane (or when $x_3 < \epsilon$, where ϵ is a threshold close to zero). The response of a particle to this collision changes the velocity of the particle. This new velocity is obtained by separating the velocity at the time of collision into two orthogonal components: the *normal component* and *tangential component* defined by

$$v_n = (N \cdot v)N \quad (3)$$

$$v_t = v - v_n \quad (4)$$

[2] In world coordinates, the $Z = 0$ plane defines the plane the reconstructed manuscript was placed onto during 3D reconstruction. Thus, reconstructed points on the surface of a flat manuscript would have $Z = 0$ coordinates.

where N is the collision plane's normal, v is the colliding particle's velocity and v_n and v_t are the respective components. In our case, these components are trivial to calculate, because the plane's normal vector is $[0\ 0\ 1]^T$, resulting in the following solutions: $v_n = [0\ 0\ v_3]^T$ and $v_t = [v_1\ v_2\ 0]^T$. If the collision is purely elastic, a particle's resulting velocity will travel in the same tangential direction and the opposite normal direction such that $v_{new} = v_t - v_n$. However, the normal direction can be dampened with a *coefficient of restitution*, k_r, such that $v_{new} = v_t - k_r v_n$, where k_r is a value from $[0-1]$. At $k_r = 0$, a particle's normal component will be ignored completely and the particle will essentially "stick" to the plane; alternatively $k_r = 1$ will cause the particle to reflect elastically. For our experiments we found $k_r = 0.1$ to be appropriate.

We note that it is possible to set the system's advancing time-step, δt, too high, such that $x_3 < 0$ for a particle. This implies that the particle has *penetrated* the collision plane, which is an undesirable effect. In this case, we restore the system to the previous time, $t-1$, and calculate a new time step such that $\delta t_{new} = \delta t_{prev}/2$, until the penetration condition is avoided.

3.4 Numerical Approach

Incorporating the internal and external forces, Barraff [1] describes the system with the following general ordinary differential equation:

$$\ddot{x} = M^{-1}\left(-\frac{\partial E}{\partial x} + F\right) \tag{5}$$

where E is a function of the internal springs and F is a function of external forces. M^{-1}, a diagonal matrix of particles $1/m$ and x, is the positional state of the particles. We solved this equation with both a simple *Euler* method and a fourth order *Runge-Kutta* integrator. Because it is easy to make the spring constant k_s too high in an effort to enforce a higher rigidity or stiffness in the model, the Euler method must take smaller time-steps. Better integrators exist and can be incorporated [1]. For our purposes, the Euler method proved the fastest, and its numerical instability was not a problem.

A document model is flattened by initializing the particle system with the described finite elements and initial conditions and applying a global force to drive the model to the plane. The process is complete when the mass-spring system's internal energy (spring forces) is minimized after collision with the $Z = 0$ plane (before collision, the internal energy is 0). Upon completion, the new position state of each particle is saved.

3.5 Creating the Restored Image

Each vertex in the quad mesh stores the coordinates of its initial 3D position, X, Y, Z ($[x_1, x_2, x_3]$ in phase space notation) in the world coordinate frame. The camera image's (u, v) coordinates can be determined by projecting the 3D point into the camera's frame by $[us\ vs\ s]^T = \tilde{P}[X\ Y\ Z\ 1]^T$, where $\tilde{P}$ is the camera's projection matrix. The matrix $\tilde{P}$ is obtained during the 3D acquisition step. After the flattening process, each vertex is associated with a new 3D point, X', Y', Z'. These new points are still in the world coordinate frame; their new position can be computed by projection into the camera frame as before, such that $[us'\ vs'\ s'] = \tilde{P}[X'\ Y'\ Z'\ 1]^T$. The restored image is created by texturing each finite element (quad) from its initial (u, v) position to the new (u', v') image coordinate position. We do not alter the pixel intensities in the original image, and therefore do not compensate for shading effects that may have been captured due to the deformed shape of the document.

4 Results

The following section reports three experiments used to gauge the effectiveness of the restoration approach. For the first two experiments, models were acquired using a Sony 1000 digital video camera (640 × 480) and an Epson Power (1024 × 768) light projector. The accuracy estimation of this setup (described in Section 2.5) is $0.31mm$. The last experiment uses a *Kontron* medical imaging camera (1996 × 1450), which is the primary imaging device at the British Library for manuscript digitization. The Kontron camera has a proprietary interface; a development kit was not available, limiting the depth acquisition portion of the capture to what is possible through a TWAIN driver. In addition to the high-resolution image capture mode, the Kontron provides a standard continuous PAL output signal, which we used for the 3D acquisition. The high resolution and PAL signal use the same optical pathway, and the two images are easily registered. Thus the high-resolution imagery is used for the texturing. A Panasonic (1024 × 768) light projector provided the structured light. We estimate the depth accuracy for the manuscript 3D models in this third experiment as $0.25mm$.

4.1 Experiment I: Pixel Distance

The first experiment is intended to quantify the ability of the mass-spring system to restore a rigidly-deformed 3D model to its original 2D planar shape. Figure 3 shows a 2D image of an original flat piece of paper with a checkerboard pattern printed on it. The flat document is imaged on the $Z = 0$ plane and removed. The image of the document before it is crumpled serves as the experimental control. The document is then crumpled by hand. The shape of this "damaged" document is acquired using the structured-light rig described in Section 2. A finite element mesh of quadrilaterals is constructed from 45 × 45 samples of the height map. This mesh is used to initialize the mass-spring particle system, which flattens the model to the $Z = 0$ plane as described in Section 3. The flattening procedure takes approx-

imately 1 minute to converge on a Dell Pentium 800MHz (512 MB RAM).

After the restored image has been constructed, we compare it with the original control image. The shadows and other shading/illumination cues on the 3D surface of the crumpled sheet are still present. Hence, we make a comparison between the control image and the restored image by comparing *features* in the two images (instead of pixels). In this case, we use the corners of the checkerboard pattern. The corners are detected using the same corner detector used by our calibration process. Because the orientations of the two images will differ slightly, the two point sets are brought into alignment by calculating an affine transformation between two point sets. Figure 3 shows the results of five experiments. The 2D points are back-projected onto the $Z = 0$ plane to provide metric measurements in the world coordinate frame.

Results from experiment I show that the restored image can be registered to the control image within half an image pixel and within $0.25mm$ in the world coordinate frame.

4.2 Experiment II: OCR Processing

The second experiment uses OCR as a metric for the quality of the restoration. A document of letters is imaged while flat, as a control image, and afterwards is crumpled. OCR is performed on the control image, the unrestored crumpled image, and the *restored* flattened image. We use a commercial package, *Readiris Pro*[8], to perform the OCR[3]. We compare the number of misses by the OCR algorithm for the two documents. A miss is defined as any letter that is misclassified and any "noise" letters that are inserted. The control image was recognized 100% accurate, i.e., 0 misses. There are 176 letters present in the document. Figure 4 shows the results. This experiment was performed five times. The crumpled image causes an error rate of 5-10%. The restored image performs nearly perfectly (1-3 misses per trial, and error rate of 1-2%), much better than the unrestored image.

4.3 Experiment III: Non-Uniform Spring Stiffness

The last experiment flattens an 11th century Medieval manuscript acquired at the British Library. Unfortunately there is no ground-truth for such an experiment. However, this experiment shows the flexibility of the mass-spring framework for restoring such data. Two different materials are present in the manuscript. The original vellum document is embedded in a paper sleeve to preserve it and allow it to be bound without directly binding the vellum. These two materials, the vellum and the paper sleeve, are quite different in their properties. Their interaction often is a cause for the overall page deformation. In such a case, an editor can experiment with the flattening process by setting different internal force coefficients for each material. We run two experiments: first, with the vellum material stiffer than the paper; and second, with the paper sleeve stiffer than the vellum material. This is done by setting the appropriate spring coefficients in these areas. Figure 5 shows the results. Notice that the difference image shows large variations in the final textures that arise from these two restorations.

[3] Readiris Pro allows a training phase, where individual letters can be trained for recognition. This procedure can be ignored and is done so for our experiments.

5 Conclusion

We have presented a framework for the restoration of non-flat documents by acquiring a 3D representation of their shape and flattening this representation via a mass-spring particle system. We make two key contributions. First, we have engineered and deployed a structured light 3D acquisition system which meets cost requirements, integrates well with existing digitization setups, is easy for non-experts to use, and yields an accuracy in the field of approximately 0.25mm. Second, we have designed a flattening algorithm that provides a general "deskewing" framework for the removal of distortion caused by the underlying non-planar shape of a document. Our experiments show we can restore rigidly deformed planar documents back to their initial position with sub-millimeter and sub-pixel accuracy in world and image space respectively. Moreover, the mass-spring particle system provides a flexible framework for addressing non-rigid and non-uniform deformation. While this work presents scholars with new tools for visualization and restoration of manuscripts, it can also be applied as a pre-processing step to improve overall performance of document analysis systems that must deal with warped and crumpled materials.

References

[1] D. Baraff and A. Witkin. Large steps in cloth simulation. In *Computer Graphics (Proc. SIGGRAPH)*, pages 43–52, August 1998.

[2] M. S. Brown and W. B. Seales. Beyond 2d images: effective 3d imaging for library materials. In *Fifth ACM Conference on Digital Library*, pages 27–36, June 2000.

[3] M. S. Brown and W. B. Seales. Digital atheneum: New approaches for preserving, restoring and analyzing damaged manuscripts. In *IEEE/ACM Joint Conference on Digital Library*, [to appear] June 2001.

[4] S. Chen and R. M. Haralick. An automatic algorithm for text skew estimation in document images using recursive morphological transforms. In *Proc. of the International Conference on Image Processing*, pages 139–143, 1994.

[5] O. Faugeras. *Three-Dimensional Computer Vision: A Geometric Viewpoint*. MIT Press, Cambridge, Massachusetts, 1993.

[6] B. Gatos, N. Papamarkos, and C. Chamzas. Skew detection in text line position determination in digitized documents. In *Pattern Recognition*, pages 30(9):1505–1519, 1997.

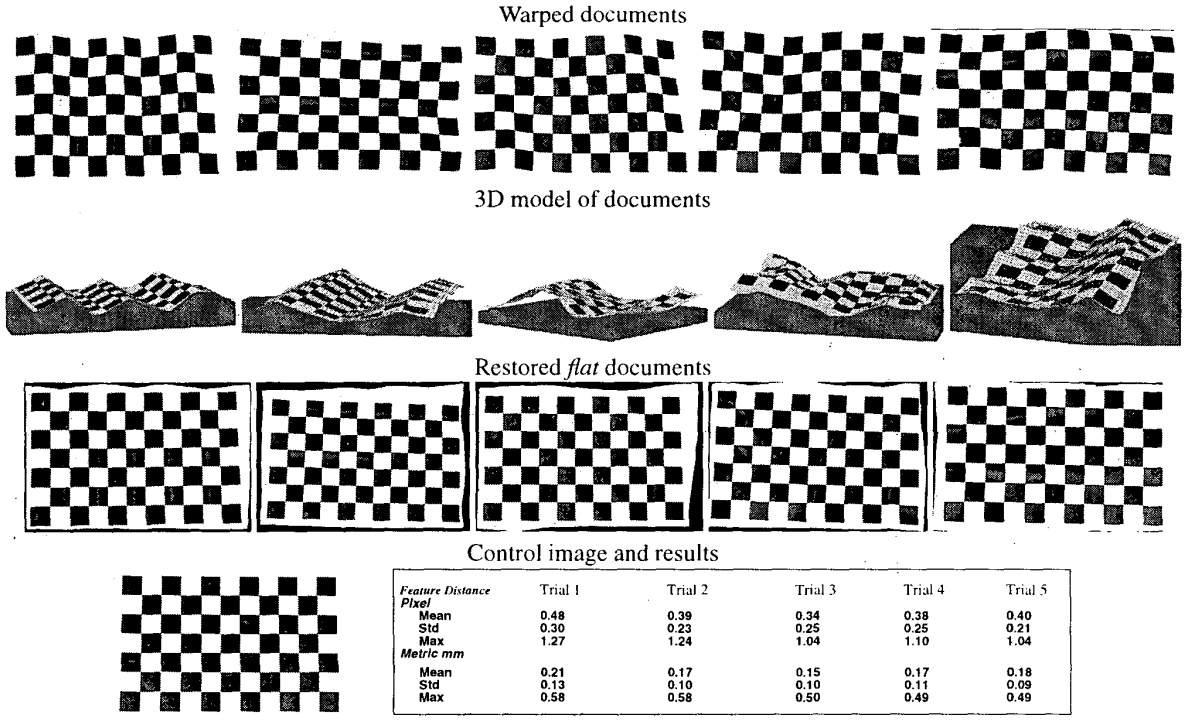

Feature Distance	Trial 1	Trial 2	Trial 3	Trial 4	Trial 5
Pixel					
Mean	0.48	0.39	0.34	0.38	0.40
Std	0.30	0.23	0.25	0.25	0.21
Max	1.27	1.24	1.04	1.10	1.04
Metric mm					
Mean	0.21	0.17	0.15	0.17	0.18
Std	0.13	0.10	0.10	0.11	0.09
Max	0.58	0.58	0.50	0.49	0.49

Figure 3: **Experiment I** Row I shows the 2D images of a crumpled document. Row II shows views of the recovered 3D models. Row III presents the restored (flattened) images. Row IV shows the experiment's control image and the pixel and metric distances between corners in the flattened images and corners in the control image.

[7] E. Horn and N. Kiryati. Toward optimal structured light patterns. In *Proceedings of the International Conference on Recent Advances in Three Dimensional Digital Imaging and Modeling*, pages 28–25, 1997.

[8] Image Recognition Integrated Systems (I.R.I.S). Readiris Pro. *Rue Du Bosquet 10, 1348 Louvain-la-Nueve - Belgium*, http://www.irislink.com.

[9] M. Kass, D. Baraff, and A. Witkin. An introduction to physically based modeling. In *SIGGRAPH Course Notes, ACM SIGGRAPH*, August 1995.

[10] L. Kitchen and A. Rosenfeld. Gray-Level Corner Detection. *Pattern Recognition Letters*, pages 1:2, 95–102, 1982.

[11] E. Lecolinet, L. Likforman-Sulem, L. Robert, F. Role, and J-L. Lebrave. An integrated reading and editing environment for scholarly research on literary works and their handwritten sources. In *Proc. of the third ACM Conference on Digital Libraries*, pages 144–151, 1998.

[12] Pavlidis, T. and Mori, S. (eds.). Optical character recognition. In *Special Issue of Proceedings of the IEEE*, pages 7(80), 1027–1209, July 1992.

[13] A. Prescott. The electronic Beowulf and digital restoration. *Literary and Linguistic Computing*, pages 12(197),185–95, 1997.

[14] Xavier Provot. Deformation constraints in a mass-spring model to describe rigid cloth behavior. In *Graphics Interface*, pages 174–155, 1995.

[15] B. Schatz and H. Chen. Digital Libraries: Technological Advances and Social Impacts. In *IEEE Computer*, pages 45–87, Feb. 1999.

[16] D. Terzopoulos and K. Fleischer. Modeling inelastic deformations: Viscoelasticity, plasticity, fracture. In *Computer Graphics (Proc. SIGGRAPH)*, pages 22:269–278, August 1988.

[17] D. Terzopoulos, J.C. Platt, and A.H. Barr. Elastically deformable models. In *Computer Graphics (Proc. SIGGRAPH)*, pages 21:205–214, 1987.

[18] T. Wada, H. Ukida, and T. Matsuyama. Shape from shading with interreflections under proximal light source: 3d shape reconstruction of unfolded book surface from a scanner image. In *Proc. International Conference of Computer Vision (ICCV'95)*, pages 66–71, 1995.

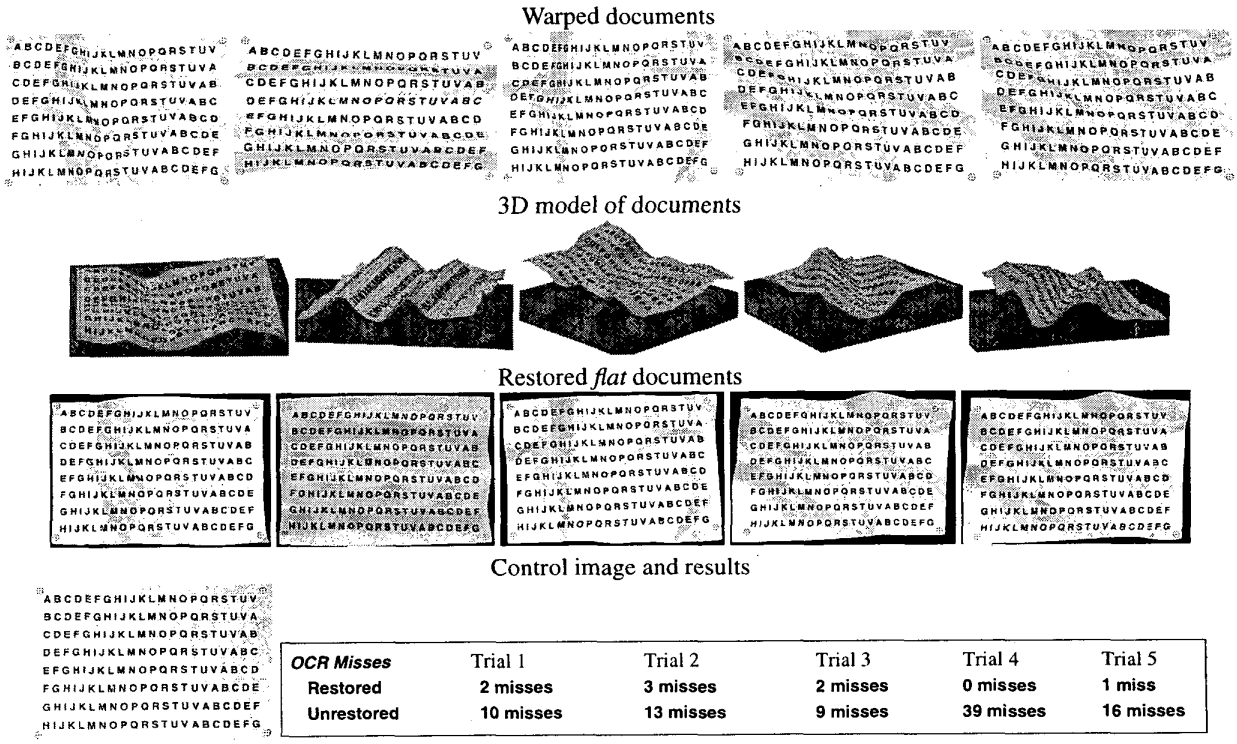

OCR Misses	Trial 1	Trial 2	Trial 3	Trial 4	Trial 5
Restored	2 misses	3 misses	2 misses	0 misses	1 miss
Unrestored	10 misses	13 misses	9 misses	39 misses	16 misses

Figure 4: Experiment II: Row I shows the 2D images of a crumpled and warped lettered document. Row II shows views of the recovered 3D models. Row III presents the restored (flattened) image. Row IV shows the control image and a table that compares the OCR results for the unrestored and the restored images.

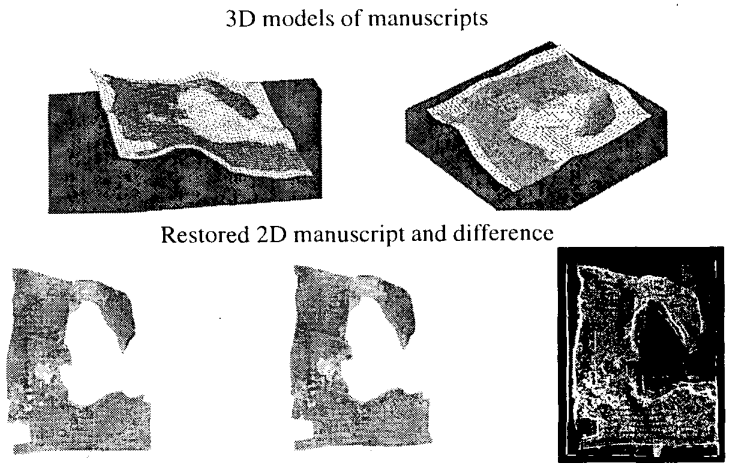

Figure 5: Experiment III: Top row shows the 3D model of a manuscript. The spring stiffness coefficients are non-uniform across the finite element mesh placed over the manuscript (see text). Middle row shows the resulting restored images and the difference between the two.